TELEVISION ANTENNAS

At the present time, the superturnstile antenna (of which the batwing antenna is a radiating element) (1), the supergain antenna (dipole antennas with a reflector plate), invented in the United States, and the Vierergruppe antenna, invented in Germany and sometimes called the *two-dipole antenna* in Japan, are widely used for very high frequency television (VHF-TV) broadcasting around the world. The superturnstile antenna (2) is used in Japan, as well as in the United States.

Figure 1 shows the appearance of the original batwing antenna, when it was first made public by Masters (1). The secret lies in its complex shape. It is called a *batwing antenna* in the United States and *Schmetterlings Antenne* (butterfly antenna) in Germany, in view of this shape.

The characteristics of the batwing antenna were calculated using the moment method proposed by Harrington (3) and experiments were conducted on this antenna. The model antenna was approximately two-fifths the size of a full-scale batwing antenna, with its design center frequency at 500 MHz.

It has been reported that for thick cylindrical antennas, a substantial effect on the current distribution appears due to nonzero current on the flat end faces. The assumption of zero current at the flat end face is appropriate for a thin cylindrical antenna; however, in the case of a thick cylindrical antenna, this assumption is not valid.

Specifically, this article applies the moment method to a full-wave dipole antenna, with a reflector plate supported by a metal bar, such as those widely used for TV and frequency modulated (FM) broadcasting (4). In the present study, the analysis is made by including the flat end-face currents. As a result, it is found that the calculated and measured values agree well, and satisfactory wideband characteristics are obtained.

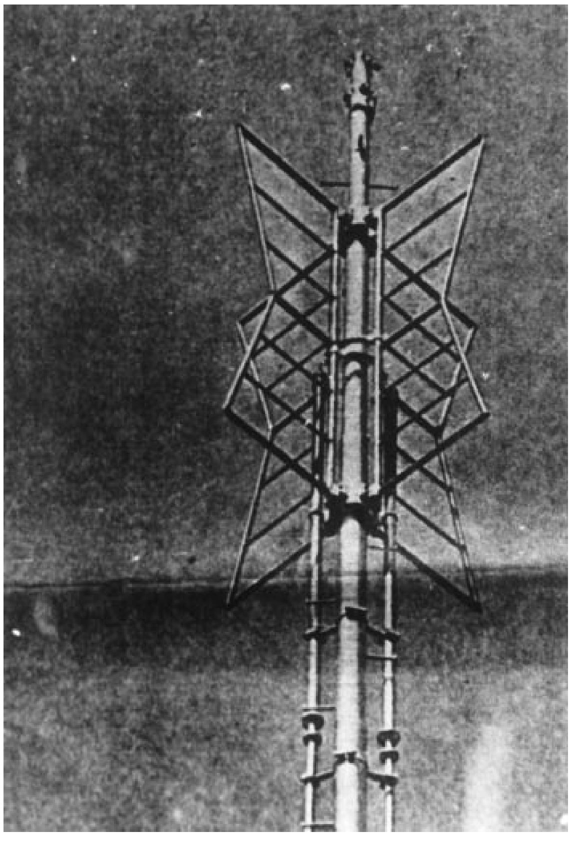

Figure 1. Historical shape of the batwing radiator.

Next, the twin-loop antennas, most widely used for ultra high frequency (UHF)-TV broadcasting, are considered. Previous researchers analyzed them by assuming a sinusoidal current distribution. Others adopted the higher order expansions (Fourier series) of the current distribution; however, their analyses did not sufficiently explain the wideband characteristics of this antenna.

This article applies the moment method to a twin-loop antenna with a reflector plate or a wire screen-type reflector plate. As for the input impedance, 2-L-type twin-loop antennas have reactance near zero [in the case where $l_1 = 0.15\ \lambda_0$, that is, where the voltage standing-wave ratio (VSWR) is nearly equal to unity]. Also, satisfactory wideband characteristics are obtained. The agreement between the measurement and the theory is quite good. Thus it may become possible in the future to improve practical antenna characteristics, based on the results obtained. Several very popular television (transmitting) antennas (5,6) were mentioned, such as slot array, normal mode helix, and V-dipole antennas.

THE BATWING ANTENNA ELEMENT

The antenna is installed around a support mast, as shown in Fig. 2, and fed from points f and f', through a jumper from a branch cable with a characteristic impedance of 72 Ω. The conducting support mast is idealized by an infinite, thin mast. The batwing antenna element is divided into 397 segments for the original type, with triangular functions as the weighting and expansion functions, and the analysis of the batwing antenna elements carried out using the Galerkin's method. The batwing antenna is fed with unit voltage. The currents flowing in each antenna conductor are calculated over a frequency range of 300 to 700 MHz.

Figure 3 illustrates these current distributions $I_i (i = 1 \sim 12)$ on the conductors at frequencies of 300, 500, and 700 MHz. Since the distribution of currents along each conductor is calculated, this allows calculation of the radiation characteristics. Figure 4 illustrates the amplitude and phase characteristics of radiation patterns in the horizontal and vertical planes. It is seen from this figure that the theoretical values agree well with the measurements.

Figure 5 illustrates the theoretical and measured input impedance of a batwing antenna mounted on an aluminum plate, 3 m × 3 m. Both curves coincide closely with each other, with the input impedance having a value close to 72 Ω, which is the proper match to the characteristic impedance of the branch cable. Vernier impedance matching is carried out in practice by connecting a metal jumper between the end of the branch cable and the feed point of the antenna element or the support mast. The feed strap's length, width, or form is varied to derive VSWR values below 1.10.

The power gain of the antenna at 500 MHz is calculated to be 3.3 dB. Figure 6 shows the gain of the antenna in the $\phi = 0°$ direction as a function of the frequency, referenced to a half-wavelength dipole. Figure 7 illustrates three-dimensional amplitude characteristics of radiation patterns in the horizontal and vertical planes at each frequency.

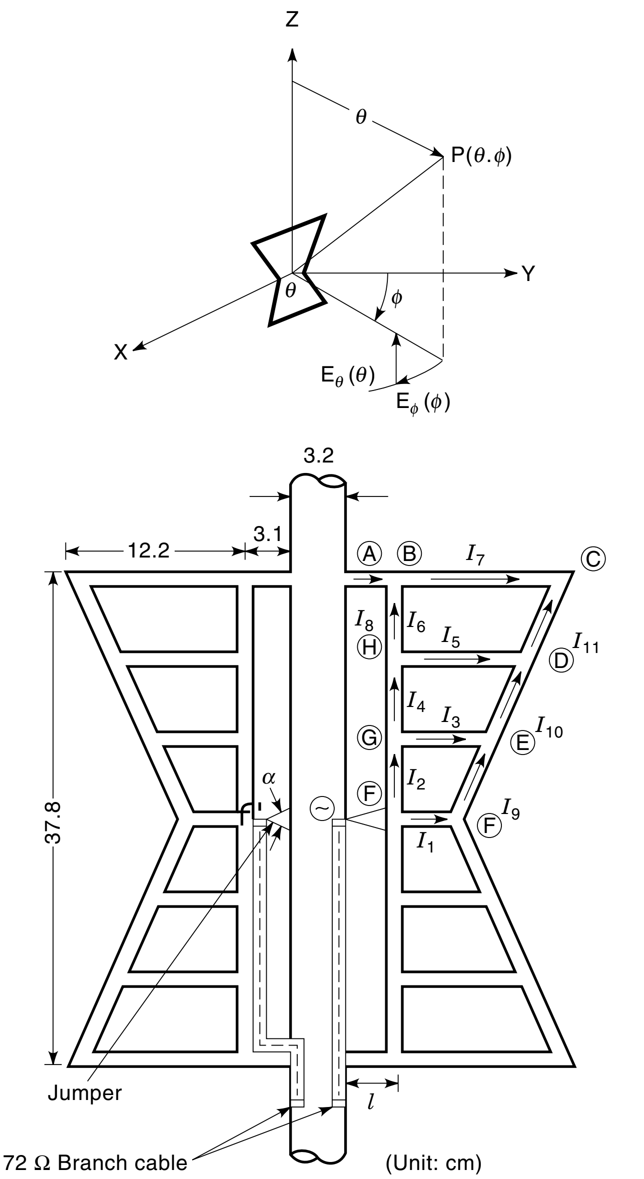

Figure 2. Construction of the model batwing antenna and its coordinate system.

THEORETICAL ANALYSIS OF METAL-BAR-SUPPORTED WIDEBAND FULL-WAVE DIPOLE ANTENNAS WITH A REFLECTOR PLATE

Wideband full-wave dipole antennas with a reflector plate supported by metal bars were invented in Germany. The construction is shown in Fig. 8. A full-wave dipole antenna is located in front of a reflector, and supported directly by a metal bar attached to a reflector. This antenna was also analyzed by the moment method described previously.

Because the supporting bar (see Fig. 8) is metallic, leakage currents may cause degradation of the radiation characteristics. To calculate these effects, the radial component of field, $E\rho$ must be taken into consideration. In other words, $E\rho$ is needed for the calculation of $Z_{m,n}$, as defined by inner products of the expansion functions on the supporting bar and weighting functions on the antenna element or on the parallel conductors. We assume the supporting bar to be separated from the feed point by a distance l_1. Also, the radius of the supporting bar is fixed at a fourth of the radius of the antenna element (i.e., at $\lambda_0/100$), and then is varied to be 0.2 λ_0, 0.25 λ_0, and 0.3 λ_0. Figures 9 to 12 indicate various calculated performance characteristics. Note that the leakage current of the supporting bar is minimized for $f/f_0 = 0.7$, and that this current is substantial at other frequencies. The current distribution is shown only for the case of $l_1 = 0.25\ \lambda_0$.

CHARACTERISTICS OF 2*L* TWIN-LOOP ANTENNAS WITH INFINITE REFLECTOR

As shown in Fig. 13, a twin-loop antenna has the loops connected by a parallel line: The 2*L*-type, 4*L*-type, and 6*L*-type

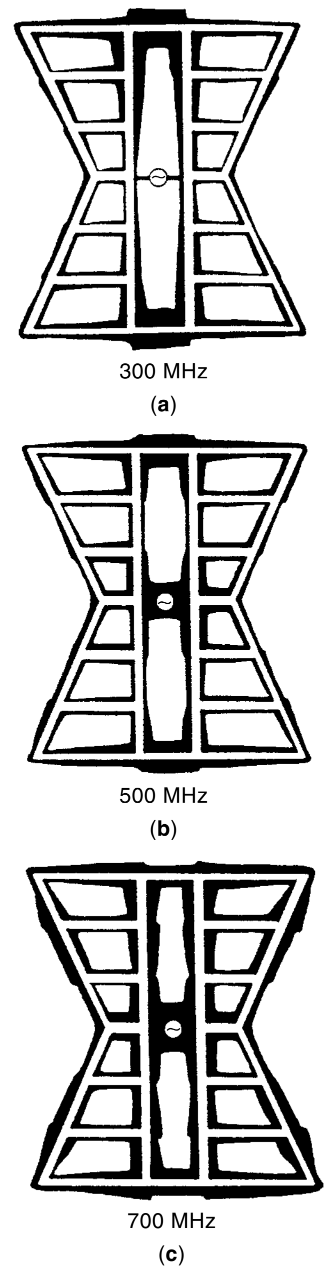

Figure 3. Amplitude characteristics of current distribution for frequency range from 300, 500, 700 MHz of shaded areas.

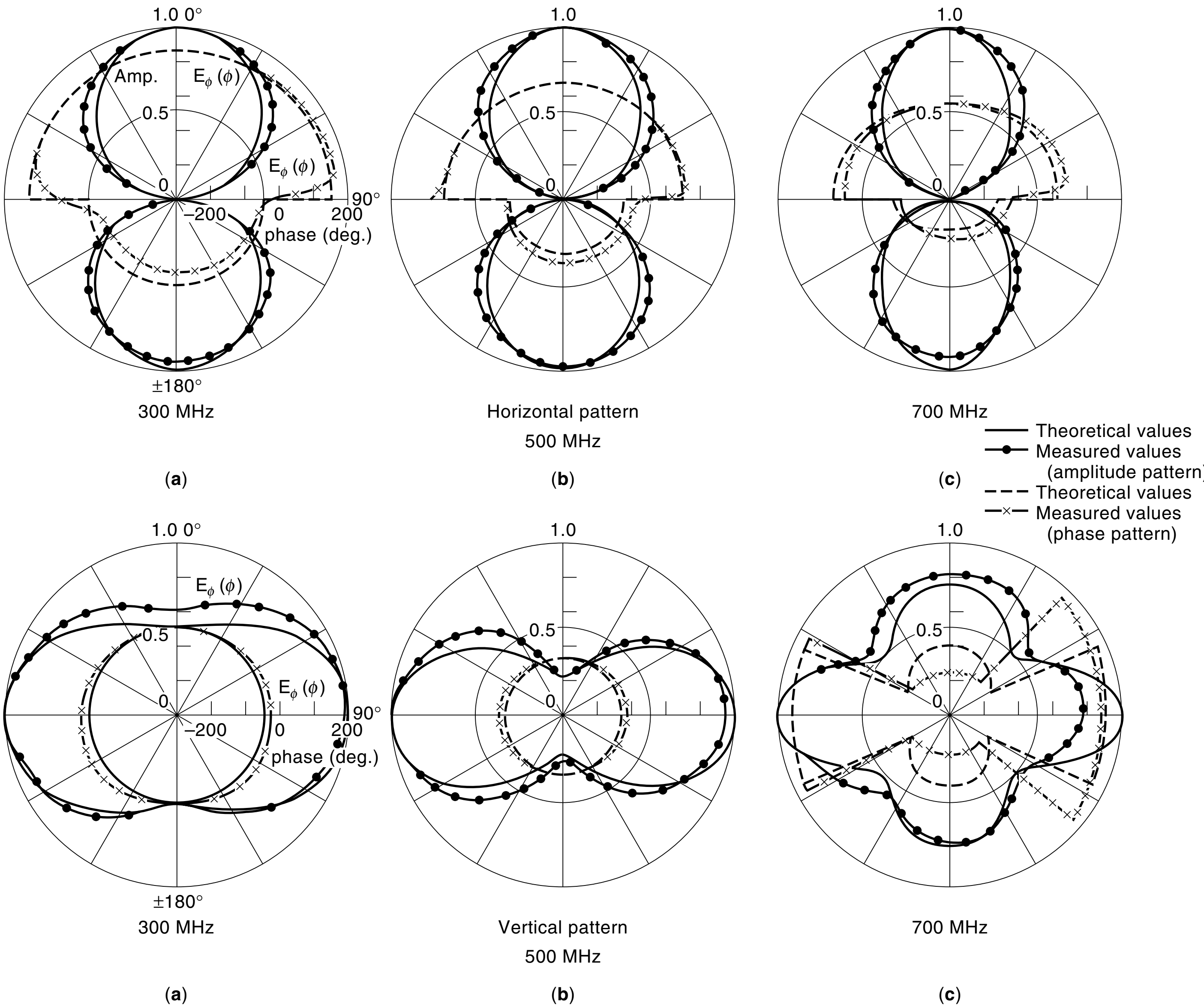

Figure 4. Amplitude and phase characteristics of radiation patterns at 300, 500, 700 MHz (with support mast).

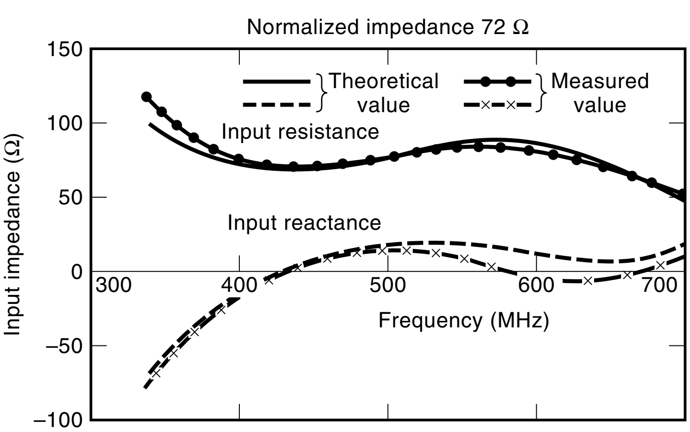

Figure 5. Theoretical and measured values of the input impedance as function of frequency (mast is infinite thin, $\alpha = 0°$).

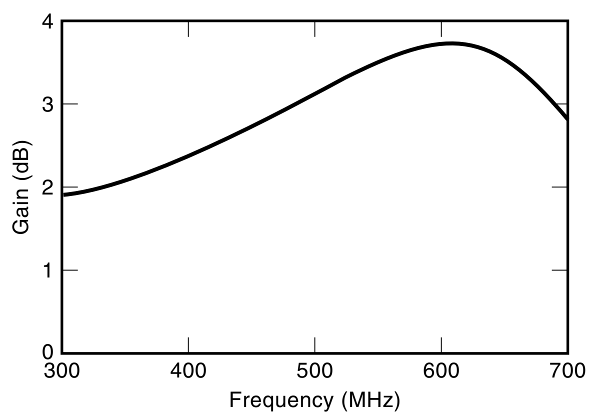

Figure 6. Batwing antenna gain with $\lambda/2$ dipole.

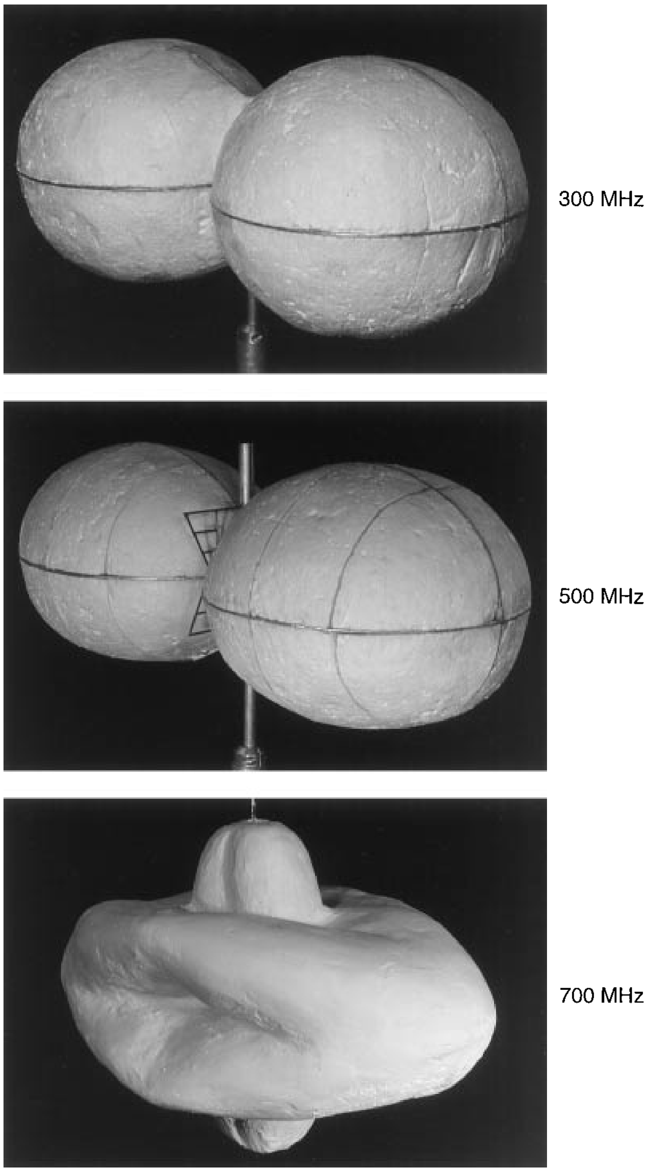

Figure 7. Three-dimension amplitude characteristics of radiation patterns at 300, 500, 700 MHz.

are used, according to the number of loops. For actual use, a reactive load is provided by the trap at the top end, which also serves as the antenna support. The dimensions used for this article are as follows: center frequency $f_0 = 750$ MHz (wavelength $\lambda_0 = 40$ cm), length of the parallel line part $2l_1 = \lambda_0/2$ ($l_1 = 10$ cm), $12 = \lambda_0/2$ ($l_2 = 20$ cm), interval of the parallel line part, $d = \lambda_0/20$ ($d = 2$ cm), loop radius $b = \lambda_0/2\pi$ ($b = 6.366$ cm), distance from the reflector to the antenna $l_3 = \lambda_0/4$ ($l_3 = 10$ cm), conductor diameter $\phi = 10$ mm, and top-end trap $l_t = 0$ to $\lambda_0/4$, changed in intervals of $\lambda_0/16$. 2L twin-loop antennas were arranged in front of an *infinite* reflector, and calculations were executed in regard to the frequency characteristics of the trap length.

The radiation pattern of the type 2L antenna is shown in Fig. 14. Up to $l_t = \lambda_0/8$, the main beam gradually becomes sharper with increasing frequency, and it can be seen that the sidelobes increase. When l_t increases in this way to $\lambda_0/8$ and $\lambda_0/4$, the directivity becomes disturbed.

Figure 14 shows $l_1 = 0.15\ \lambda_0$ and $l_1 = 0.25\ \lambda_0$ characteristics of the radiation pattern in a polar display. The antenna gain for both lengths ($l_1 = 0.15\ \lambda_0$ and $l_1 = 0.25\ \lambda_0$) shows a small change of approximately 9.5–8.5 dB.

The input impedance has a value very close to 50 Ω, essentially the same as the characteristic impedance of the feed cable. As for the input impedance, the 2L twin-loop antenna has reactance nearest zero (for the case where $l_1 = 0.15\ \lambda_0$), that is, the VSWR is nearly equal to unity.

In the above calculation, the reflector was considered to be an infinite reflector, and the effect of the reflector on the antenna elements was treated by the image method. In the case of practical antennas, however, it is the usual practice to make the reflector finite, or consisting of several parallel conductors. Therefore, a calculation was executed for a reflector in which 21 linear conductors replaced the infinite reflector, as shown in Fig. 15.

The results are shown along with those for the infinite-reflector case. Based on these results, it was concluded that no significant difference was observed in input impedance and gain between the infinite reflector case and the case where the reflector consisted of parallel conductors.

The wire screen-type of reflector plate had a height of 3 λ_0 (120 cm), a width of λ_0 (40 cm), and a wire interval of 0.15 λ_0 (6 cm). The radiation pattern is shown in Fig. 16. With regard to the pattern in the horizontal plane, no difference was found in comparison with an infinite reflector, but a backlobe of approximately −16 dB exists to the rear of the reflector. The same figure also shows the phase characteristics. With regard to the pattern in the vertical plane, the phase shows a large change where the pattern shows a cut.

SEVERAL POPULAR TRANSMITTING ANTENNAS

Slot Antennas

Both resonant and nonresonant end-fed arrays of slots are used for TV broadcasting. The resonant arrays are restricted

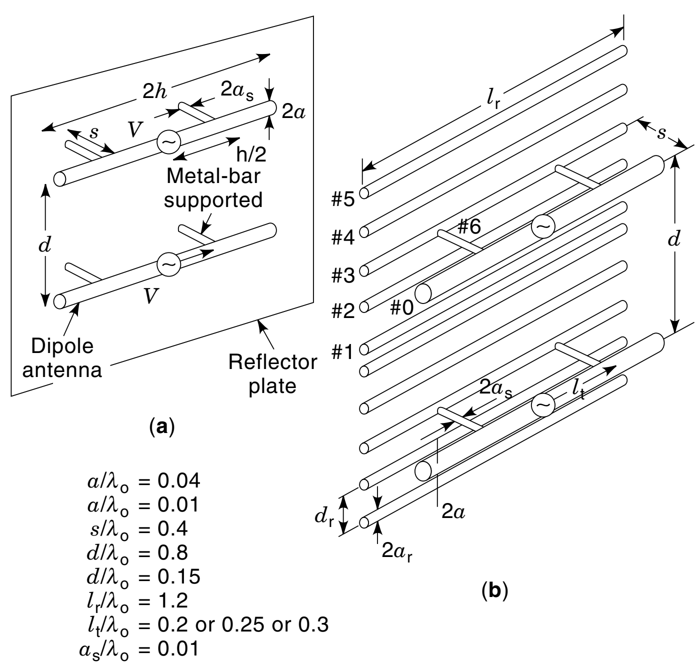

Figure 8. Metal-bar supported wideband full-wave dipole antennas with a reflector plate.

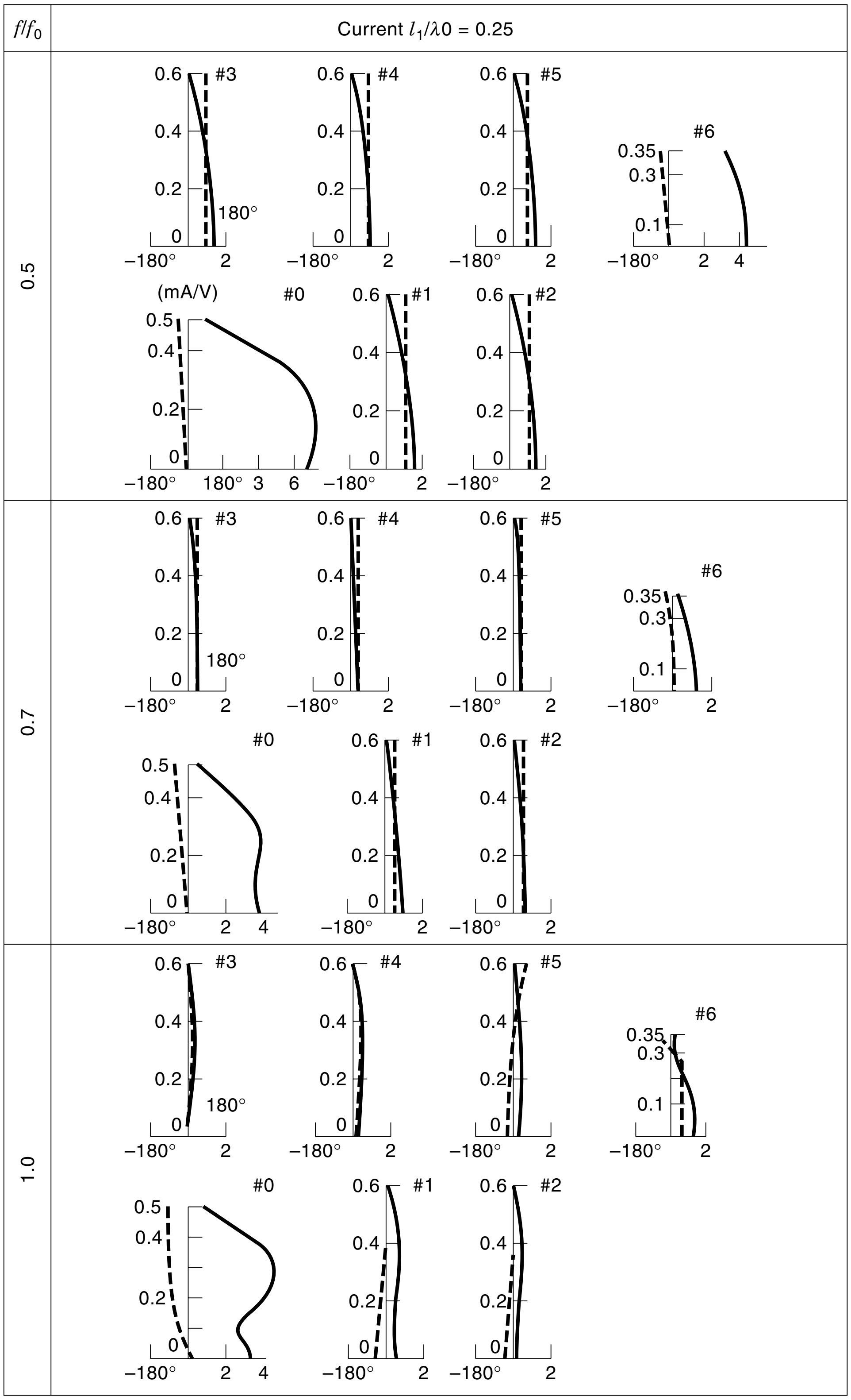

Figure 9. Current distribution of metal-bar supported full-wave dipole antennas (two-bay) with a wire screen-type reflector plate.

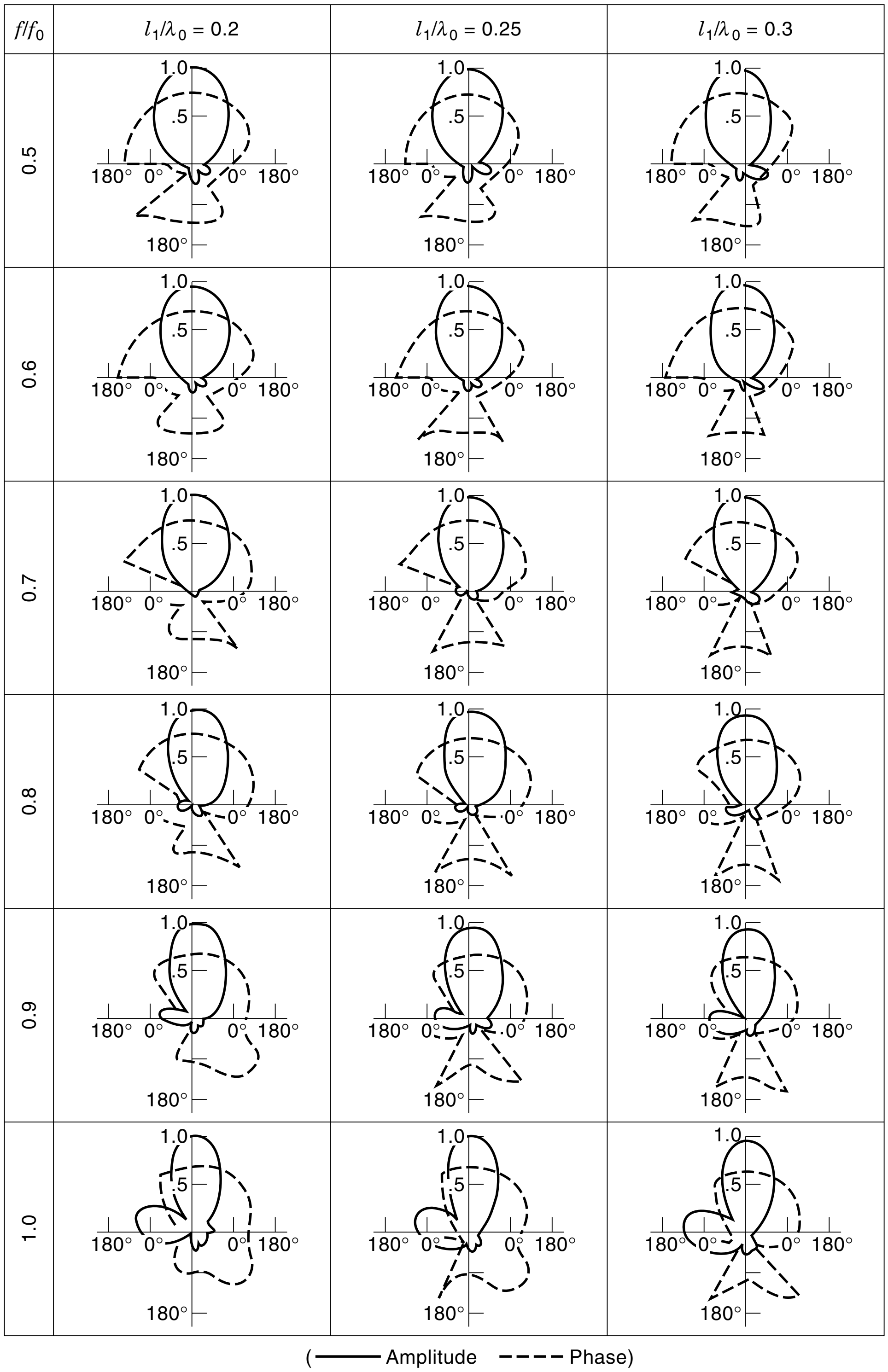

Figure 10. Radiation pattern of metal-bar supported full-wave dipole antennas (two-bay) with a wire screen-type reflector plate.

to UHF applications because of their limited bandwidth. The traveling-wave slot antenna illustrated in Fig. 17 is a large end-fed coaxial transmission line with a slotted outer conductor. The slots are arranged in pairs at each layer, with the pairs separated by a quarter wavelength along the length of the antenna. Adjacent pairs occupy planes at right angles to each other. The slot pairs, which are approximately one-half wavelength long, are fed out of phase by the coaxial line by capacitive probes projecting radially inward from one side of each slot so as to produce a figure-eight pattern. The probes

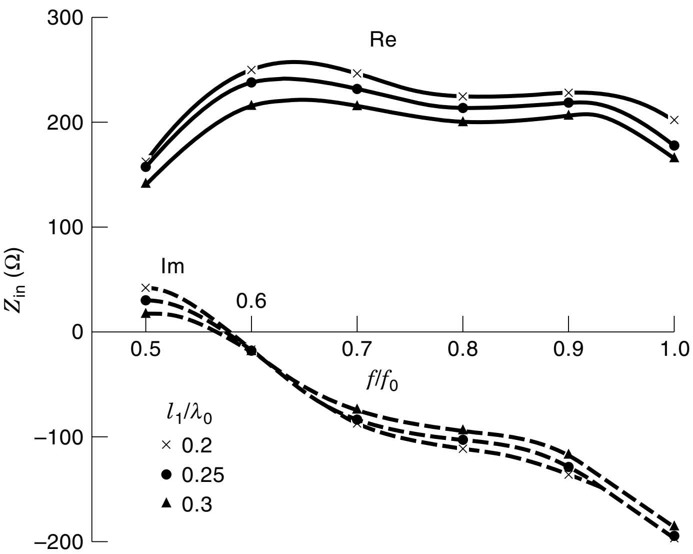

Figure 11. Input impedance characteristics of metal-bar supported full-wave dipole antennas (two-bay) with a wire screen-type reflector plate.

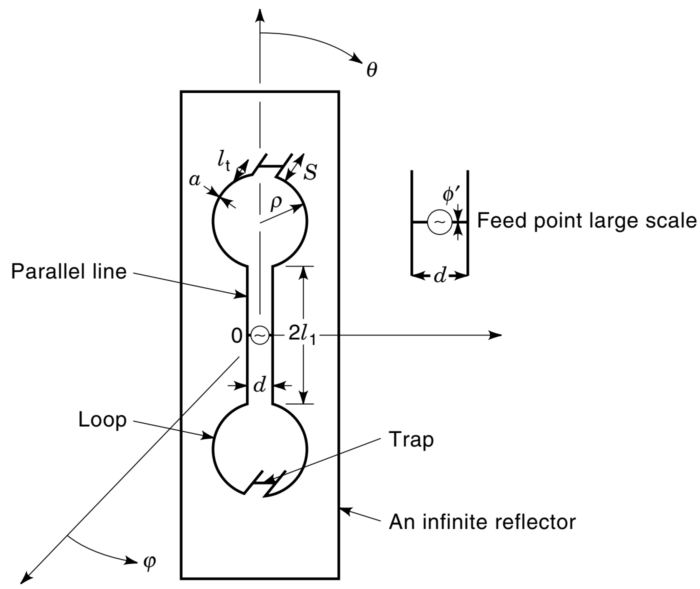

Figure 13. Structure of $2L$-type twin-loop antenna and its coordinate system for analysis.

are placed on opposite sides of adjacent in-line slots which are spaced one-half wavelength to provide in-phase excitation. The quarter-wavelength separation of layers in conjunction with the space-quadrature arrangement of successive layers of slots effects a turnstile-type feed which produces a horizontally polarized azimuth pattern with a circularity of ± 1 dB for VHF applications. An equal percentage of the power in the coaxial line is fed to each layer of slots, which results in an exponential aperture distribution that provides null fill.

Reflections from adjacent layers tend to cancel, which allows the traveling-wave operation. The top slots are strongly coupled to the line to reduce reflections. For high-gain applications, one-half of the slots may be eliminated, resulting in a one-wavelength spacing of in-line slots. The standing-wave antenna consists of layers or bays of one or more axial slots spaced by one wavelength and fed by a coaxial line with the slotted pipe forming the outer conductor. Azimuth patterns are controlled by the number of slots per bay. One slot per bay produces a skull-shaped pattern, two slots a peanut-shaped pattern, and three slots a trilobe pattern. Four or more slots per bay are usually required for an ominidirectional pattern with a circularity of ± 1 dB. A typical omnidirectional pattern is shown in Fig. 18.

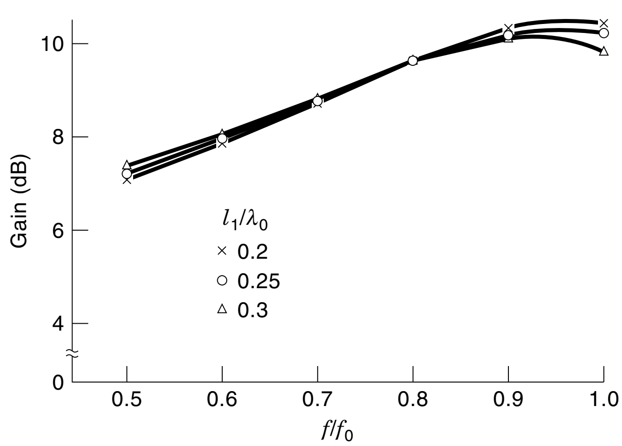

Figure 12. Gain of metal-bar supported full-wave dipole antennas (two-bay) with a wire screen-type reflector plate.

Helix Antennas

Figure 19 shows a single bay of a single-arm right-hand and left-hand helix fed in phase at the center so that the vertically polarized components of the two helices cancel in the broadside direction. The pitch angle is about 12° so that the vertically polarized radiation from each helix is about 10 dB down from the horizontally polarized radiation, which produces about 0.5 dB loss in gain due to cross-polarization radiation. Since the beam of each helix scans about 2.7° per 1% change in frequency, the bay length is limited to about six wavelengths. Sidefire helical antenna pattern is shown in Fig. 20.

V-Shaped Antennas

The multi-V antenna has been designed especially to mount on the side of existing towers which are used for standard broadcast radiators or TV supporting towers. The multi-V antenna array (Fig. 21) consists of a number of V elements stacked vertically to provide power gain in the horizontal plane and vertical directivity. The resulting horizontal radiation pattern is essentially omnidirectional. The pattern remains approximately circular when side-mounted on a tower having a uniform cross section with 2 ft on a side.

The bays, or V's, are so designed that the input impedance of each pair is 50 Ω, enabling them to be fed by standard coaxial transmission lines. The feed system enables an even number of bays from two to eight to be employed to obtain power gains ranging from 1.6 to 7.3. The design is such that it is necessary to tune the antenna at the factory for the desired

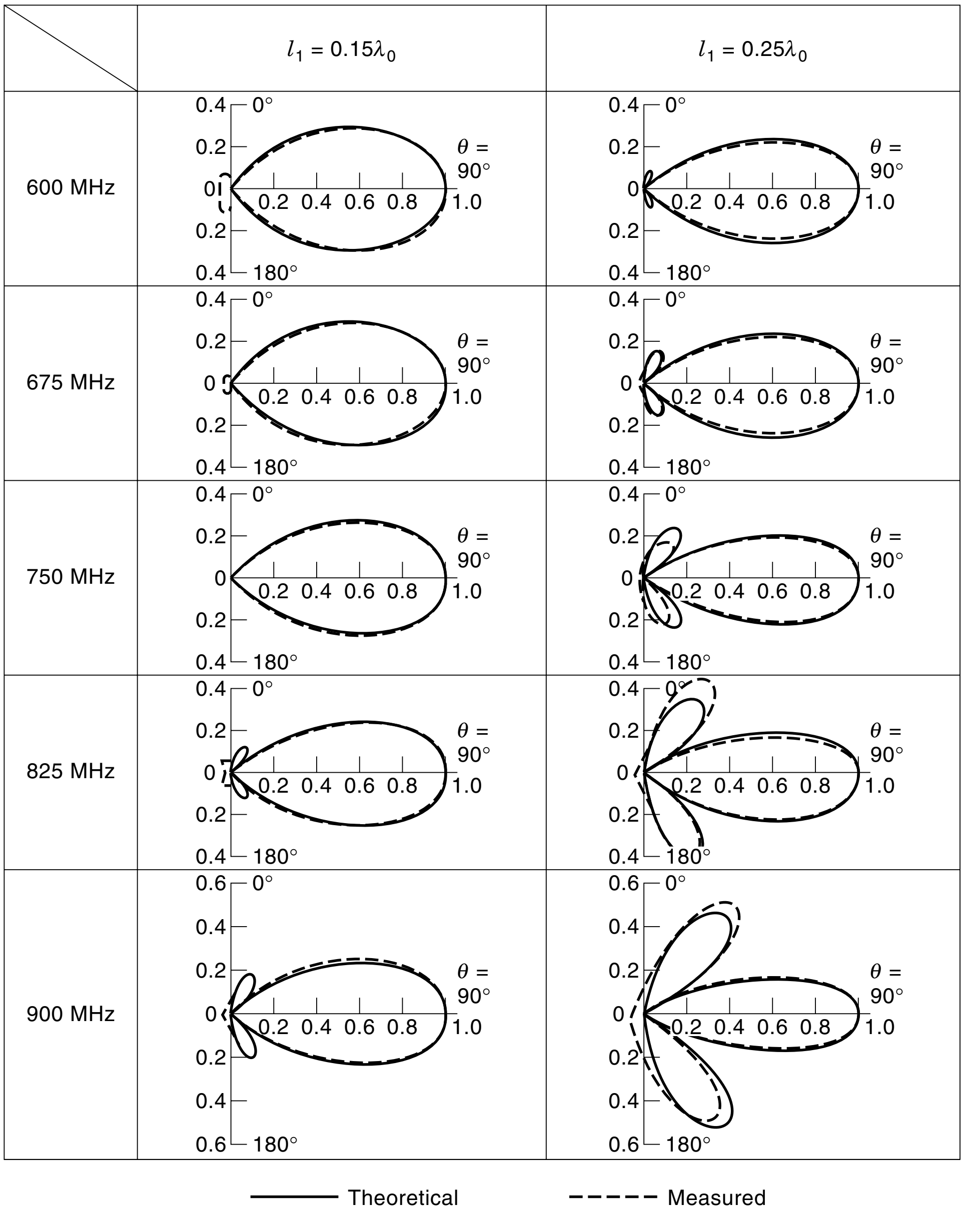

Figure 14. Vertical radiation pattern of 2L-type twin-loop antenna.

frequency. It is very simple, with one feed point per bay and a maximum of four power-dividing elements for an eight-bay array. The radiating elements are grounded for maximum lightning protection. Figure 22 shows the four bay V antenna pattern for various values of space.

CONCLUSION

Previous researchers (1,2) have analyzed batwing antennas by approximating the current distribution as a sinusoidal distribution. Wideband characteristics are not obtained with a sinusoidal current distribution. In this article, various types of modified batwing antennas, as the central form of the superturnstile antenna system, were analyzed theoretically with the aid of the moment method. The results were compared with measurements, in order to examine the performance of the antenna elements in detail.

It is also evident from this research that the shape of the jumper has a remarkable effect on the reactance of the input impedance, and that the distance between the support mast and the antenna element also markedly influences the resistance of this impedance. Thus, a satisfactory explanation is given with regard to the matching conditions. As a result, it was found that the calculated and measured values agree well, and satisfactory wideband characteristics are obtained.

Next an analytic method and calculated results for the performance characteristics of a thick cylindrical antenna were presented. The analysis used the moment method and takes the end face currents into account. The calculated results were compared with measured values, demonstrating the accuracy of the analytic method.

Using this method, a full-wave dipole antenna with a reflector supported by a metal bar was analyzed. The input impedance was measured for particular cases, thus obtaining the antenna dimensions for which the antenna input imped-

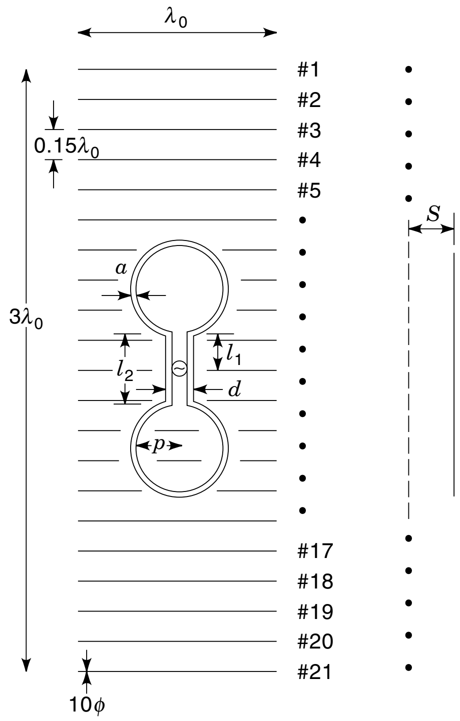

Figure 15. Structure of $2L$-type twin-loop antenna with a wire screen-type reflector plate.

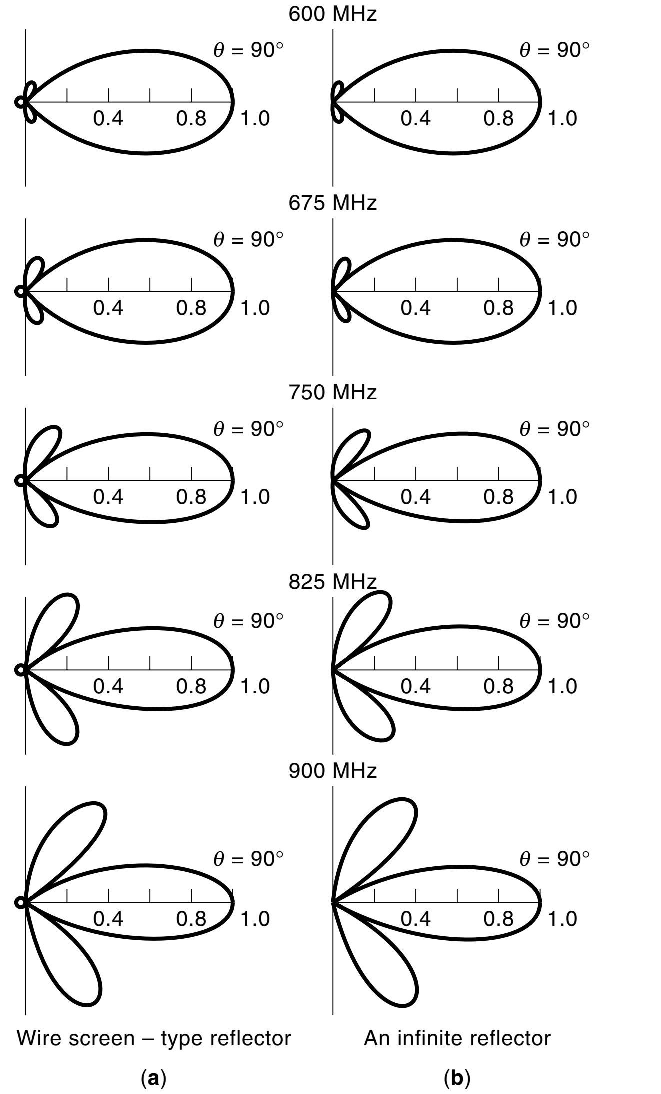

Figure 16. Comparison between characteristics of $2L$-type twin-loop antenna with a wire screen-type reflector and with an infinite reflector.

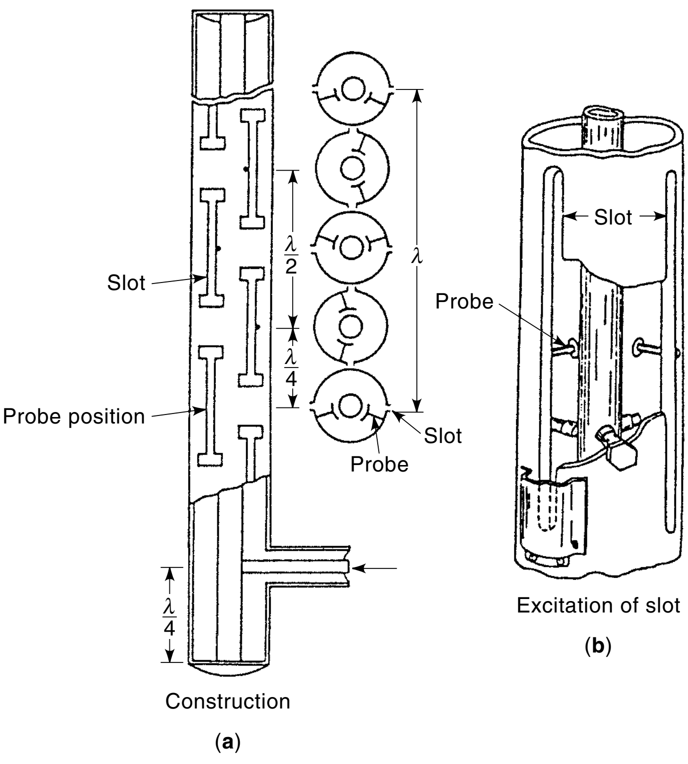

Figure 17. The traveling-wave slot antenna.

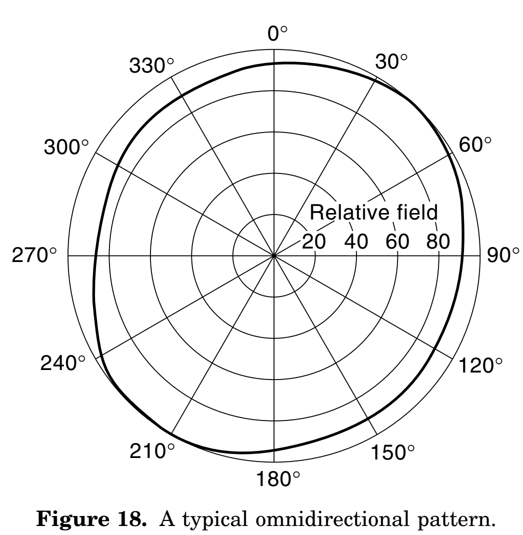

Figure 18. A typical omnidirectional pattern.

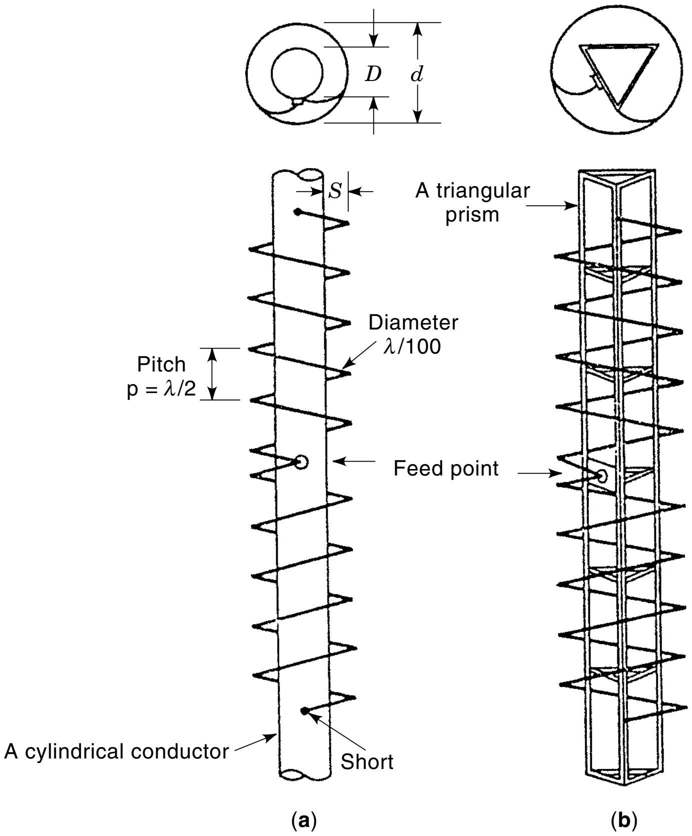

Figure 19. A sidefire helical antenna.

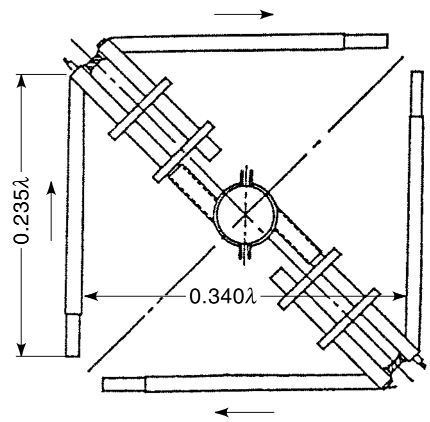

Figure 21. The construction of V-shaped antenna.

ance permits broadband operation. In conclusion, wideband characteristics are not obtained with a one-bay antenna. The wideband characteristic is obtained by means of the mutual impedance of the two-bay arrangement. In the frequency region of $f/f_0 = 0.7$, the resistance of the input impedance is considered to be constant. In this case, the leakage current to the support bar is small. With regard to the radiation pattern, it was seen that a degradation of characteristics was caused by the metal support bar.

It is noted that the present method should be similarly useful for analyzing antennas of other forms where the end face effect is not negligible.

Next, the twin-loop antennas were considered for use as wideband antennas. The analysis results for $2L$ type showed

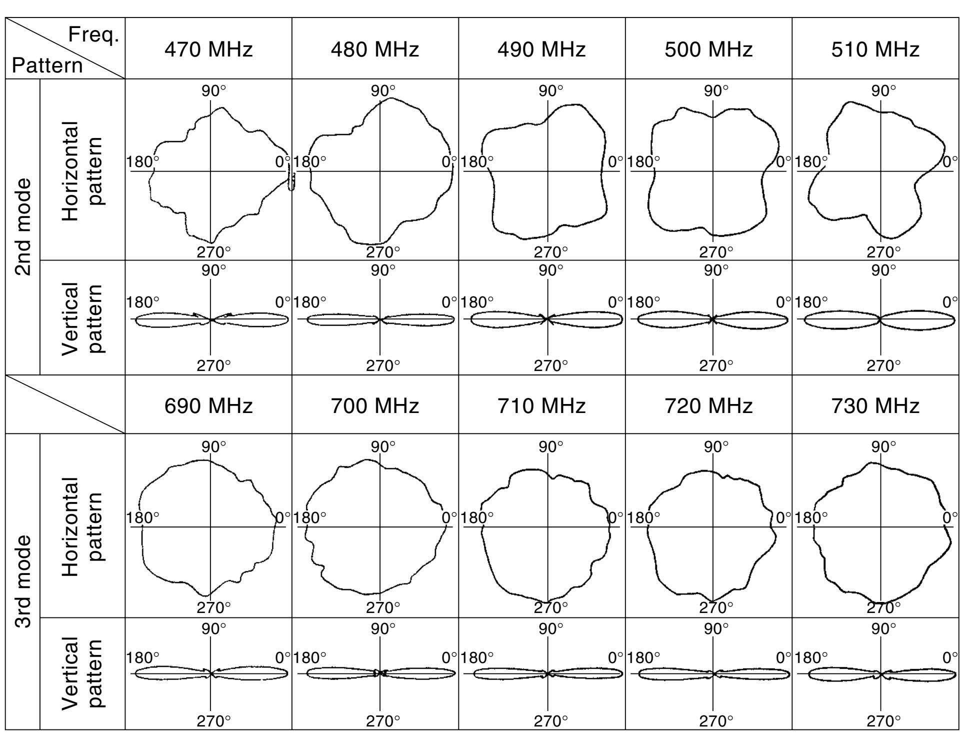

Figure 20. The horizontal and vertical pattern of sidefire helical antenna.

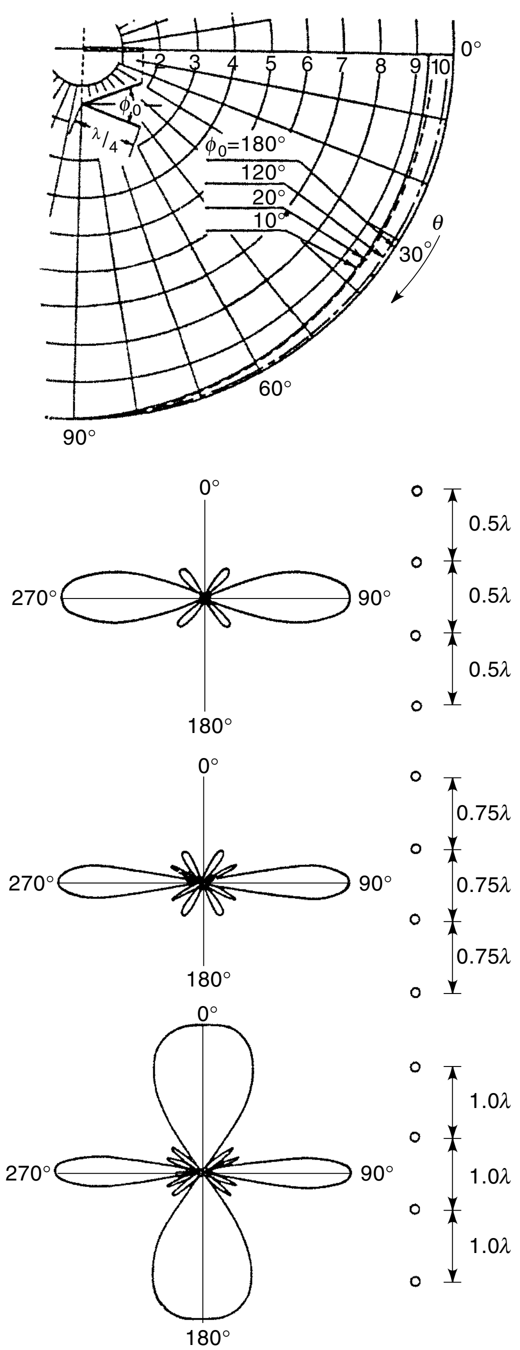

Figure 22. Vertical and horizontal pattern of V-shaped antenna.

that the change in the characteristics with a change in frequency becomes more severe with increasing trap length l_t, and the bandwidth becomes small, while a short trap length l_t shows a small change and a tendency for the bandwidth to become wide. For $l_t = 0$, a wide bandwidth for pattern and gain was obtained for the 2L type. The input impedance has a value very close to 50 Ω, essentially the same as the characteristic impedance of the feed cable over a very wide frequency range. Thus, a satisfactory explanation was given with regard to the matching conditions. Popular television antennas cover the properties of many basic types of antennas which are the mainstream of antenna technology. It has been reported here that a rigorous theoretical analysis has been achieved almost 30 years after the invention of these VHF–UHF antennas.

BIBLIOGRAPHY

1. R. W. Masters, The super turnstile. *Broadcast News,* **42**: 1946.
2. Y. Mushiake, (ed.), *Antenna Engineering Handbook.* The OHM-Sha, Ltd., 1980 (in Japanese).
3. R. F. Harrington, *Field Computation By Moment Method,* New York: Macmillan, 1968.
4. W. Berndt, Kombinierte Sendeantennen Fur Fernseh-und UKW-runfunk (Teil II), *Telefunken-Zeitung, Jahrgang, Heft. 26,* **101**: 268, 1953.
5. Y. T. Lo and S. W. Lee, Antenna Handbook, New York: Van Nostrand Reinhold, 1988.
6. R. C. Johnson and H. Jasik, Antenna Engineering Handbook, New York: McGraw Hill, 1984.

HARUO KAWAKAMI
Antenna Giken Corporation

TELEVISION BROADCASTING BY DIRECT SATELLITE.

See DIRECT SATELLITE TELEVISION BROADCASTING.